Hindawi Publishing Corporation
Journal of Applied Mathematics
Volume 2012, Article ID 659872, 17 pages
doi:10.1155/2012/659872

Research Article

Nonlinear Dynamics of an Electrorheological Sandwich Beam with Rotary Oscillation

Kexiang Wei,[1] Wenming Zhang,[2] Ping Xia,[1] and Yingchun Liu[1]

[1] *Department of Mechanical Engineering, Hunan Institute of Engineering, Xiangtan 411101, China*
[2] *State Key Laboratory of Mechanical System and Vibration, Shanghai Jiao Tong University, Shanghai 200240, China*

Correspondence should be addressed to Kexiang Wei, kxwei@hnie.edu.cn

Received 29 August 2012; Accepted 28 November 2012

Academic Editor: Vasile Marinca

The dynamic characteristics and parametric instability of a rotating electrorheological (ER) sandwich beam with rotary oscillation are numerically analyzed. Assuming that the angular velocity of an ER sandwich beam varies harmonically, the dynamic equation of the rotating beam is first derived based on Hamilton's principle. Then the coupling and nonlinear equation is discretized and solved by the finite element method. The multiple scales method is employed to determine the parametric instability of the structures. The effects of electric field on the natural frequencies, loss factor, and regions of parametric instability are presented. The results obtained indicate that the ER material layer has a significant effect on the vibration characteristics and parametric instability regions, and the ER material can be used to adjust the dynamic characteristics and stability of the rotating flexible beams.

1. Introduction

The dynamics of rotating flexible beams have been the subject of extensive research due to a number of important applications in engineering such as manipulators, helicopters, turbine blades, and so forth. Much research about the dynamic modeling and vibration characteristics of fixed-shaft rotating beams has been published in recent decades. Chung and Yoo [1] investigated the dynamic characteristics of rotating beams using finite element method (FEM) and obtained the time responses and distribution of the deformations and stresses at a given rotating speed. The nonlinear dynamics of a rotating beam with flexible root attached to a rotating hub with elastic foundation has been analyzed by Al-Qaisia [2]. He discussed the effect of root flexibility, hub stiffness, torque type, torque period and

excitation frequency and amplitude on the dynamic behavior of the rotating beam-hub. Lee et al. [3] investigated divergence instability and vibration of a rotating Timoshenko beam with precone and pitch angles. The nonlinear modal analysis of a rotating beam has been studied by Arvin and Bakhtiari-Nejad [4]. The stability and some dynamic characteristics of the nonlinear normal modes such as the phase portrait, Poincare section, and power spectrum diagrams have been inspected. But most research to date has examined only the effects of steady velocity on the vibration characteristics of the flexible beam, without considering the dynamic characteristics of speed variation of beams. Rotating flexible beams with variable speeds, such as manipulators, demonstrate complex dynamic characteristics because of changes in angular velocity. The beam can suffer from dynamic instability under certain movement parameters. Therefore, the vibration stability of flexible beams with variable angular velocity has attracted increasing attention in recent years. Abbas [5] studied the dynamics of rotating flexible beams fixed on a flexible foundation, and using FEM analyzed the effects of rotation speed and flexible foundation on the static buckling load and region of vibration instability. Young and Lin [6] investigated the parametrically excited vibration of beams with random rotary speed. Sinha et al. [7] analyzed the dynamic stability and control of rotating flexible beams with different damping coefficients and boundary conditions. Chung et al. [8] studied the dynamic stability of a fixed-shaft cantilever beam with periodically harmonic swing under different swing frequencies and speeds. Turhan and Bulut [9] studied the vibration characteristics of a rotating flexible beam with a central rigid body under periodically variable speeds, and simulated the dynamic stability of the system under different movement parameters. Nonlinear vibration of a variable speed rotating beam has been analyzed by Younesian and Esmailzadeh [10]. They investigated the parameter sensitivity and the effect of different parameters including the hub radius, structural damping, acceleration, and the deceleration rates on the vibration amplitude.

Electrorheological (ER) materials are a kind of smart material whose physical properties can be instantaneously and reversibly controlled with the application of an electric field. These unusual properties enable ER materials to be employed in numerous potential engineering applications, such as shock absorbers, clutch/brake systems, valves and adaptive structures. One of the most commonly studied ER structures is the ER sandwich beam, in which an ER material layer is sandwiched between two containing surface layers [11]. These sandwich structures have the adaptive control capability of varying the damping and stiffness of the beam by changing the strength of the applied electric field. Since Gandhi et al. [12] first proposed the application of ER fluids to adaptive structures, much has been achieved in the vibration control of beams [13–15]. More recently, the dynamic stability problems of ER sandwich beams have attracted some attention. Yeh et al. [16] studied the dynamic stability problem of an ER sandwich beam subjected to an axial dynamic force. They found that the ER core had a significant effect on the dynamic stability regions. Yeh and Shih [17] investigated the critical load, parametric instability, and dynamic response of a simply supported ER adaptive beam subjected to periodic axial force. However, research into the application of ER materials to vibration control of rotating motion beams is rare. In our previous work [18], the feasibility of applying ER fluids to the vibration control of rotating flexible beams was discussed. Results demonstrated that the vibration of the beam caused by the rotating motion at different rotation speeds and acceleration could be quickly suppressed by applying electric fields to the ER material layer. When the angular velocity of the rotating ER sandwich beam is variable, the rotating beam would suffer from parametric instability at some critical movement parameters. In order to successfully apply ER materials to the vibration control of rotating beams and optimize the control effects, it is needed to

investigate the nonlinear dynamic characteristics and vibration stabilities of the rotating ER sandwich beam.

In this paper, the dynamic characteristics and parametric instability of a rotating ER sandwich beam with rotary oscillation is investigated. Assuming the ER sandwich beam to rotate around a fixed axis with time-varying harmonic periodic motion, the rotating ER sandwich beam is regarded as a parametrically excited system. Based on Hamilton's principle and finite element method (FEM), the governing equations of the rotating beam are obtained. The multiple scales method is employed to determine the regions of instability for simple and combination resonances. The effects of electric field on the natural frequency, loss factor, and regions of parametric instability are investigated. The results of the stability analysis are verified by investigating the time responses of the ER sandwich beam.

2. Properties of ER Fluids

ER fluids behave as Newtonian fluids in the absence of an electric field. On application of an electric field, their physical appearance changes to resemble a solid gel. However, their rheological response changes before and after the yield point. Due to this difference in rheological behavior before and after the yield point, the rheology of ER fluids is approximately modeled in pre-yield and post-yield regimes (Figure 1). The pre-yield regime can be modeled by a linear viscoelastic model, and the post-yield regime be modeled by the Bingham plastic model.

Existing studies [16, 17, 19, 20] demonstrate that the ER materials behave as linear visco-elastic properties when they are filled in a sandwich beam configuration. So the shear stress τ is related to the shear strain γ by the complex shear modulus G^*,

$$\tau = G^*\gamma. \tag{2.1}$$

The complex shear modulus G^* is a function of the electric field strength applied on the ER fluids, and can be written in the form

$$G^* = G_1 + G_2 i = G_1(1 + \eta i), \tag{2.2}$$

where G_1 is the storage modulus, G_2 is the loss modulus, $\eta = G_2/G_1$ is the loss factor, and $i = \sqrt{-1}$. So sandwich beams filled with ER fluids behave like visco-elastic damping beams with controllable shear modulus.

3. Finite Element Modeling of Rotating ER Sandwich Beams

Because ER materials exhibit linear shear behavior at small strain levels similar to many visco-elastic damping materials, it is found that the models developed for the viscoelastically damped structures were potentially applicable to ER materials beams [20]. So in the present study, the finite element model for a rotating beam with a constrained damping layer [21, 22] is adopted to model the rotating ER sandwich beam.

3.1. Basic Kinematic Relationships of the Rotating Beam

The structure of an ER sandwich beam is shown in Figure 2. The ER material layer is sandwiched between two elastic surface layers. The beam with a length L and width b rotates in a horizontal plane at an angular velocity $\dot{\theta}$ about the axis Y.

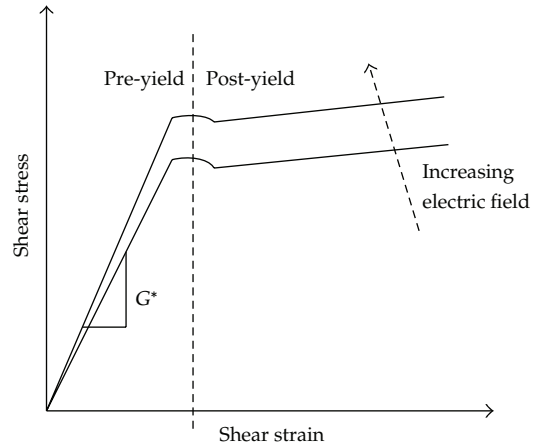

Figure 1: The shear stress-shear strain relationship of ER fluids.

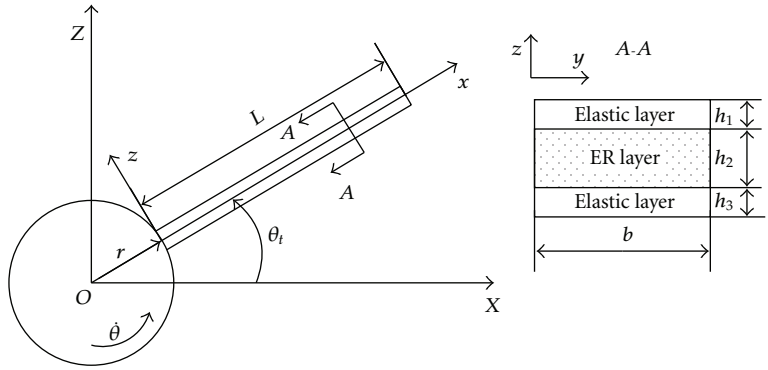

Figure 2: Rotating sandwich beam filled with ER fluid core.

It is assumed that no slipping occurs at the interface between the elastic layer and the ER fluid layer, and the transverse displacement w in a section does not vary along the beam's thickness. From the geometry of the deflected beam (Figure 3), the shear strain γ and longitudinal deflection u_2 of the ER fluid layer can be expressed as [11]

$$\begin{aligned} \gamma &= \frac{u_1 - u_3}{h_2} + \frac{h}{h_2} w_{,x}, \\ u_2 &= \frac{u_1 + u_3}{2} + \frac{h_1 - h_3}{4} w_{,x}, \end{aligned} \tag{3.1}$$

with

$$h = h_2 + \frac{(h_1 + h_3)}{2}, \tag{3.2}$$

where u_k $(k = 1, 2, 3)$ are the longitudinal displacements of the mid-plane of the kth layer; w is the transverse displacements of the beam, and subscript $(, x)$ denotes partial differentiation

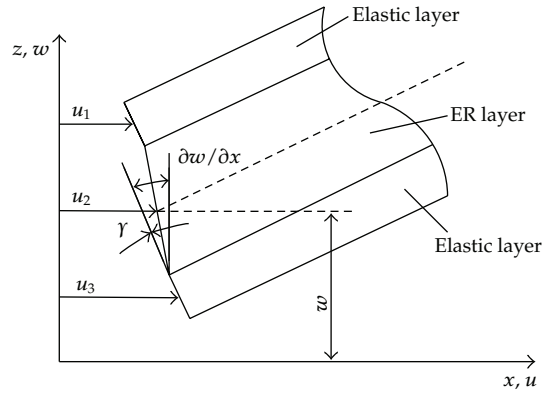

Figure 3: Kinematic relationships of deflected beam.

with respect to coordinate x; h_k $(k = 1,2,3)$ is the thickness of the kth layer; and $k = 1,2,3$ denote the upper face layer, the ER core layer, and the lower face layer, respectively.

3.2. Governing Equations

The kinetic energy for the rotating ER sandwich beam can be expressed as

$$T = \frac{1}{2}\int_0^L \sum_{k=1}^{3} \rho_k A_k \dot{u}_k^2 \mathrm{d}x + \frac{1}{2}\int_0^L \sum_{k=1}^{3} \rho_k A_k \dot{w}^2 \mathrm{d}x, \tag{3.3}$$

where ρ_k and A_k $(k = 1,2,3)$ are the density and cross-section area of the kth layer; L is the length of beam.

Assuming the shear strains in the elastic surface layers as well as the longitudinal and transverse stresses in the ER fluid layer are negligible, the strain energy of the system can be expressed as

$$U_1 = \frac{1}{2}\int_0^L \left(E_1 A_1 u_{1,x}^2\right)\mathrm{d}x + \frac{1}{2}\int_0^L \left(E_3 A_3 u_{3,x}^2\right)\mathrm{d}x + \frac{1}{2}\int_0^L (E_1 I_1 + E_3 I_3) w_{,xx}^2 \mathrm{d}x + \frac{1}{2}\int_0^L G^* A_2 \gamma^2 \mathrm{d}x, \tag{3.4}$$

where E_k $(k = 1,3)$ is the Young's modulus of the upper and lower surface layers, respectively; I_k $(k = 1,3)$ is the moment of inertia of the upper and lower surface layers, respectively; $G^* = G_1 + G_2 i$ is the complex shear modulus of the ER fluid; γ is the shear strain of the ER material layer.

The potential energies attributable to centrifugal forces are written as [21, 22]

$$U_2 = \frac{1}{2}\int_0^L P(x,t) w_{,x}^2 \mathrm{d}x \tag{3.5}$$

with

$$P(x,t) = A_t \rho_t \dot{\theta}^2 \left[r(L-x) + \frac{1}{2}\left(L^2 - x^2\right)\right], \tag{3.6}$$

where $\dot{\theta}$ is the rotating speed, A_t is the cross-section of the sandwich beam, ρ_t is the density of the system, x is the distance from the fixed end of the beam to any section on which centrifugal forces are acting, r is the hub radius.

The work done by external forces is exerted by the rotational torque τ and the external distributed force acting on the beam. In this study, only the transverse load q is considered. The total work by the external forces can be expressed as

$$W = \tau\theta + \int_0^L qbw\mathrm{d}x. \tag{3.7}$$

The governing equations of the rotating ER sandwich beam are obtained by applying Hamilton's principle

$$\int_{t_1}^{t_2} \delta(T - U + W)\mathrm{d}t = 0. \tag{3.8}$$

3.3. Finite Element Discretization

The finite element method (FEM) is used to discretize the rotating ER sandwich beam in this study. The elemental model presented here consists of two nodes, each of which has four degrees of freedom. Nodal displacements are given by

$$\mathbf{q}_i = \left\{u_{1j} \;\; u_{3j} \;\; w_j \;\; w_{j,x} \;\; u_{1k} \;\; u_{3k} \;\; w_k \;\; w_{k,x}\right\}^T, \tag{3.9}$$

where j and k are elemental node numbers, and u_1, u_3, w, $w_{,x}$ denote the longitudinal displacement of upper layer and lower layer, the transverse displacement, and the rotational angle, respectively.

The deflection vector $\{u_1 \; u_2 \; u_3 \; w \; w_{,x}\}$ can be expressed in terms of the nodal deflection vector $\mathbf{q}_i$ and finite element shape functions

$$\left\{u_1 \;\; u_2 \;\; u_3 \;\; w \;\; w_{,x}\right\} = \left\{\mathbf{N}_1 \;\; \mathbf{N}_2 \;\; \mathbf{N}_3 \;\; \mathbf{N}_4 \;\; \mathbf{N}_{4,x}\right\}^T \mathbf{q}_i, \tag{3.10}$$

where $\mathbf{N}_1$, $\mathbf{N}_2$, $\mathbf{N}_3$, and $\mathbf{N}_4$ are the finite element shape functions and are given by

$$\begin{aligned}
\mathbf{N_1} &= \left[1-\zeta \;\; 0 \;\; 0 \;\; 0 \;\; \zeta \;\; 0 \;\; 0 \;\; 0\right], \\
\mathbf{N}_2 &= \frac{1}{2}\left(\mathbf{N}_1 + \mathbf{N}_3 + \frac{h_1 - h_3}{2}\mathbf{N}_{4,x}\right), \\
\mathbf{N}_3 &= \left[0 \;\; 1-\zeta \;\; 0 \;\; 0 \;\; 0 \;\; \zeta \;\; 0 \;\; 0\right], \\
\mathbf{N}_4 &= \left[0 \;\; 0 \;\; 1-3\zeta^2+2\zeta^3 \;\; \left(\zeta - 2\zeta^2 + \zeta^3\right)L_i \;\; 0 \;\; 0 \;\; 3\zeta^2 - 2\zeta^3 \;\; \left(-\zeta^2 + \zeta^3\right)L_i\right],
\end{aligned} \tag{3.11}$$

with $\zeta = x/L_i$ and L_i is the length of the element.

Substituting (3.10) into (3.3)–(3.7) and Hamilton's principle (3.8), the element equations of the rotating sandwich beam can be obtained as follows

$$\mathbf{M}^e\ddot{\mathbf{q}}^e + 2\dot{\theta}\mathbf{C}^e\dot{\mathbf{q}}^e + \left[\mathbf{K}_1^e + \dot{\theta}^2\left(\mathbf{K}_2^e - \mathbf{M}^e\right) - \ddot{\theta}\mathbf{C}^e\right]\mathbf{q}^e = \mathbf{F}^e, \tag{3.12}$$

where $\mathbf{M}^e$, $\mathbf{C}^e$, $\mathbf{K}_1^e$, and $\mathbf{K}_2^e$ are the element mass, the element gyroscopic, the element stiffness, and the element motion-induced stiffness matrices of the rotating beam, respectively; $\mathbf{F}^e$ is the element load vector. These element matrices and vector may be expressed as

$$\begin{aligned}
\mathbf{M}^e &= \int_0^{L_i} \sum_{k=1}^{3} \left[\rho_k A_k \left(\mathbf{N}_k^T \mathbf{N}_k + \mathbf{N}_4^T \mathbf{N}_4\right)\right] \mathrm{d}x, \\
\mathbf{C}^e &= \int_0^{L_i} \left[\sum_{k=1}^{3} \rho_k A_k \left(\mathbf{N}_k^T \mathbf{N}_4 - \mathbf{N}_k \mathbf{N}_4^T\right)\right] \mathrm{d}x, \\
\mathbf{K}_1^e &= \int_0^{L_i} \sum_{k=1}^{3} \left(E_k A_k \mathbf{N}_{k,x}^T \mathbf{N}_{k,x} + E_k I_k \mathbf{N}_{4,xx}^T \mathbf{N}_{4,xx}\right) \mathrm{d}x \\
&\quad + \int_0^{L_i} \frac{G^* A_2}{h_2^2} (\mathbf{N}_1 - \mathbf{N}_3 + h\mathbf{N}_{4,x})^T (\mathbf{N}_1 - \mathbf{N}_3 + h\mathbf{N}_{4,x}) \mathrm{d}x, \\
\mathbf{K}_2^e &= \frac{1}{2} \int_0^{L_i} \left(\sum_{k=1}^{3} \rho_k A_k\right) \left[L^2 - (x_i + x)^2\right] \mathbf{N}_{4,x}^T \mathbf{N}_{4,x} \mathrm{d}x \\
&\quad + r \int_0^{L_i} \left(\sum_{k=1}^{3} \rho_k A_k\right) [L - (x_i + x)] \mathbf{N}_{4,x}^T \mathbf{N}_{4,x} \mathrm{d}x, \\
\mathbf{F}^e &= \int_0^{L_i} \left\{\sum_{k=1}^{3} \left[\rho_k A_k \dot{\theta}^2 (r + x_i + x) \mathbf{N}_k^T\right] - \sum_{k=1}^{3} \left[\rho_k A_k \ddot{\theta} (r + x_i + x) \mathbf{N}_4^T\right]\right\} \mathrm{d}x + \sum_{i=1}^{n} \mathbf{F}_{qi}.
\end{aligned} \tag{3.13}$$

Assembling each element, the global equation of the rotating ER sandwich beam is

$$\mathbf{M}\ddot{\mathbf{q}} + 2\dot{\theta}\mathbf{C}\dot{\mathbf{q}} + \left[\mathbf{K_1} + \dot{\theta}^2(\mathbf{K_2} - \mathbf{M}) - \ddot{\theta}\mathbf{C}\right]\mathbf{q} = \mathbf{F}, \tag{3.14}$$

where $\mathbf{M}$ is the global mass matrix; $\mathbf{C}$ is the global gyroscopic matrices; $\mathbf{K_1}$ is the global stiffness matrices, which is complex due to the complex shear modulus G^* of the ER material; $\mathbf{K_2}$ is the global motion-induced stiffness matrices, and $\mathbf{F}$ is the global load vector.

Since the first longitudinal natural frequency of a beam is far separated from the first transverse natural frequency, the gyroscopic coupling terms in (3.14) could be assumed negligible and ignored [23]. With this assumption, (3.14) can be simplified as

$$\mathbf{M}\ddot{\mathbf{q}} + \left[\mathbf{K_1} + \dot{\theta}^2(\mathbf{K_2} - \mathbf{M})\right]\mathbf{q} = \mathbf{F}. \tag{3.15}$$

It is assumed that the ER sandwich beam rotates around a fixed axis for a sinusoidal periodic swing and the speed is

$$\dot{\theta} = \dot{\theta}_0 \sin \tilde{\omega} t, \tag{3.16}$$

where $\dot{\theta}_0$ is the maximum angular speed of the rotating beam and $\tilde{\omega}$ is the frequency of the swing. Substituting (3.16) into (3.15), the dynamic equation for the rotating ER sandwich beam without applied external forces can be obtained as

$$\mathbf{M}\ddot{\mathbf{q}} + \mathbf{K_1}\mathbf{q} + \left(\dot{\theta}_0 \sin \tilde{\omega} t\right)^2 (\mathbf{K_2} - \mathbf{M})\mathbf{q} = 0. \tag{3.17}$$

Assume $\mathbf{\Phi}$ is the normalized modal matrix of $\mathbf{M}^{-1}\mathbf{K_1}$, (3.17) can be transformed to the following N coupled Mathieu equations ifa linear transformation $\mathbf{q} = \mathbf{\Phi\xi}$ is introduced and only the homogeneous part of the equation:

$$\ddot{\xi}_i + \omega_i^2\xi_i + \dot{\theta}_0^{*2}\sin^2(\tilde{\omega}t)\sum_{k=1}^{N} h_{ik}\xi_k = 0, \tag{3.18}$$

where ω_i^2 are the eigenvalues of $\mathbf{M}^{-1}\mathbf{K_1}$ and h_{ik} are the elements of the complex matrix $\mathbf{H} = -\mathbf{\Phi}^{-1}\mathbf{M}^{-1}(\mathbf{K_2} - \mathbf{M})\mathbf{\Phi}$. ω_i and h_{ik} are written as

$$\omega_i = \omega_{i,R} + \mathrm{i}\omega_{i,I}, \qquad h_{ik} = h_{ik,R} + \mathrm{i}h_{ik,I}, \quad \mathrm{i} = \sqrt{-1}. \tag{3.19}$$

4. Stability Analysis

Equation (3.18) represents a typical parametrically excited system because the last term on its left-hand side is a periodic function of time. When the system parameters reach special resonance conditions, the rotating beam will suffer divergence instability [24]. The determination problem of these conditions is called dynamic stability analysis. In this section, stability of the solutions of (3.18) will be studied by multiscale method.

It is assumed that the dimensional maximum angular speed of the ER rotating beam can be expressed as a function of a small value $\varepsilon < 1$:

$$\dot{\theta}_0^{*2} = 4\varepsilon. \tag{4.1}$$

Based on the multi-scale method, the solution for (3.18) can be written as

$$\xi_i(t,\varepsilon) = \xi_{i0}(T_0, T_1, \ldots) + \varepsilon\xi_{i1}(T_0, T_1, \ldots) + \cdots, \quad i = 1\cdots n, \tag{4.2}$$

where ξ_{i0} and ξ_{i1} represent the displacement function of fast and slow scales, respectively; $T_0 = t$ is the fast time scale; and $T_1 = \varepsilon t$ is the slow time scale.

Substituting (4.1) and (4.2) into (3.18), and comparing the same-order exponent, we obtain

$$\varepsilon^0 : D_0^2\xi_{i0} + \omega_i^2\xi_{i0} = 0, \tag{4.3}$$

$$\varepsilon^1 : D_0^2\xi_{i1} + \omega_i^2\xi_{i1} = -2D_0D_1\xi_{i0} + \left(e^{2\mathrm{i}\tilde{\omega}T_0} + e^{-2\mathrm{i}\tilde{\omega}T_0} - 2\right)\sum_{k=1}^{n} h_{ik}\xi_{k0}, \tag{4.4}$$

where $D_n = \partial/\partial T_n$ $(n = 0, 1)$, h_{ik} is the uniterm at row i and column k in matrix $\mathbf{H}$. It should be noted that the effective excitation frequency is $2\tilde{\omega}$ in (4.4), which is originated from $\sin^2(\tilde{\omega}t)$ of (3.18). This is different from the equation of motion for an axially oscillating cantilever beam, in which has $\sin\tilde{\omega}t$ instead of $\sin^2(\tilde{\omega}t)$ [9].

Using the first order approximation, the general solution of (4.3) can be expressed in the form

$$\xi_{i0} = A_i(T_1, T_2)e^{\mathrm{i}\omega_i T_0} + \overline{A}_i(T_1, T_2)e^{-\mathrm{i}\omega_i T_0}, \tag{4.5}$$

where $A_i(T_1, T_2)$ is the complex function of slow time scale, and $\overline{A}_i(T_1, T_2)$ denotes the complex conjugate of $A_i(T_1, T_2)$.

The solution of (4.5) is substituted into (4.4) to obtain

$$D_0^2\xi_{i1} + \omega_i^2\xi_{i1} = -2\mathrm{i}\omega_i D_1 A_i e^{\mathrm{i}\omega_i T_0} + \sum_{k=1}^{n} h_{ik}A_k\left[e^{\mathrm{i}(\omega_k+2\tilde{\omega})T_0} + e^{\mathrm{i}(\omega_k-2\tilde{\omega})T_0} - 2e^{\mathrm{i}\omega_k T_0}\right] + \mathrm{cc}, \tag{4.6}$$

where cc represents the complex conjugate of all previous items. The complex functions Ai should be chosen to satisfy the conditions that ξ_{i1} is bounded. If the terms on the right-hand side of (4.6) have the excitation frequency ω_i, resonance occurs because the excitation frequency coincides with the natural frequency. These terms, called the secular terms, should be eliminated from (4.6). So the frequency of perturbation $2\tilde{\omega}$ needs to be checked for its nearness to the individual natural frequency as well as their combinations. To this order of approximation, there are three main categories of simple and combination resonances [25]. Their respective dynamic stability behaviours will be analyzed below.

(a) *Combination Resonance of Sum Type*

If the variation frequency $2\tilde{\omega}$ approaches the sum of any two natural frequencies of the system, summation parametric resonance may occur. The nearness of $2\tilde{\omega}$ to $(\omega_{p,R} + \omega_{q,R})$ can be expressed by introducing a detuning parameters σ defined by

$$\tilde{\omega} = \frac{1}{2}\left(\omega_{p,R} + \omega_{q,R}\right) + \frac{1}{2}\varepsilon\sigma, \tag{4.7}$$

where $\omega_{p,R}$ and $\omega_{q,R}$ are, respectively, the pth and qth natural frequency of the ER rotating beam.

Substituting (4.7) into (4.6), the condition required to eliminate secular terms in (4.6) can be obtained as

$$\begin{aligned} 2\mathrm{i}\omega_p D_1 A_p + 2h_{pp}A_p - h_{pq}\overline{A}_q e^{\mathrm{i}[\sigma T_1 - (\omega_{p,I}+\omega_{q,I})T_0]} &= 0, \\ 2\mathrm{i}\omega_q D_1 A_q + 2h_{qq}A_q - h_{qp}\overline{A}_q e^{\mathrm{i}[\sigma T_1 - (\omega_{p,I}+\omega_{q,I})T_0]} &= 0, \end{aligned} \tag{4.8}$$

where $\overline{A}_q$ and $\overline{A}_q$ are the complex conjugates of A_p and A_q, respectively. It should be remarked that the ω_i and h_{ik} $(i = p, q)$ in (4.8) are complex due to the complex shear modulus G^* of the ER materials layer, which are shown in (3.19).

From the condition that nontrivial solutions of (4.8) should be bounded, the boundaries of the unstable regions in this case are given by [9, 22]

$$\tilde{\omega} = \frac{1}{2}\left(\omega_{p,R} + \omega_{q,R}\right) \pm \frac{\left(\omega_{p,I} + \omega_{q,I}\right)}{4\left(\omega_{p,I}\omega_{q,I}\right)^{1/2}}\left[\frac{\left(\varepsilon\omega_{01}\right)^2\left(h^*_{pq,R}h^*_{qp,R} + h^*_{pq,I}h^*_{qp,I}\right)}{\omega_{p,R}\omega_{q,R}} - 16\omega_{p,I}\omega_{q,I}\right]^{1/2}, \tag{4.9}$$

where, $\omega_{p,R}$ and $\omega_{q,I}$ are, respectively, the real and imaginary components of the system's complex eigenvalues; and $h^*_{ij,R}$ and $h^*_{ij,I}$ respectively represent the real and imaginary components of h^*_{ij}.

When $p = q$, (4.9) can be simplified into the critical condition for instability of order n harmonic resonance,

$$\tilde{\omega} = 2\omega_{p,R} \pm \frac{1}{2}\left[\frac{(\varepsilon\omega_{01})^2\left[\left(h^*_{pp,R}\right)^2 + \left(h^*_{pp,I}\right)^2\right]}{\left(\omega_{p,R}\right)^2} - 16\left(\omega_{p,I}\right)^2\right]^{1/2}. \tag{4.10}$$

(b) *Combination Resonance of Difference Type*

When the excitation frequency $2\tilde{\omega}$ varies around the difference between the natural frequencies at orders p and q, this phenomenon is called the combination resonance of difference type. Its boundary condition of instability can be obtained by changing the sign of ω_i in the situation above. The boundary curve of the corresponding stability and instability curves is

$$\tilde{\omega} = \omega_{p,R} - \omega_{q,R} \pm \frac{\left(\omega_{p,I} + \omega_{q,I}\right)}{4\left(\omega_{p,I}\omega_{q,I}\right)^{1/2}}\left[\frac{(\varepsilon\omega_{01})^2\left(h^*_{pq,R}h^*_{qp,R} - h^*_{pq,I}h^*_{qp,I}\right)}{\omega_{p,R}\omega_{q,R}} - 16\omega_{p,I}\omega_{q,I}\right]^{1/2}. \tag{4.11}$$

(c) *No-Resonance Case*

Consider the case that the excitation frequency $2\tilde{\omega}$ is far away from $(\omega_{p,R}\pm\omega_{q,R})$ for all possible positive integer values of p and q. In this case, the condition required to eliminate the secular terms in (4.6) is

$$D_1 A_i = 0, \quad i = 1 \cdots n. \tag{4.12}$$

So the particular solution of (4.6) is

$$\begin{aligned}\xi_{i1} = & -\omega_0 \sum_{k=1}^{n} h_{ik}A_k\left[\frac{e^{\mathrm{i}(\omega_k+2\tilde{\omega})T_0}}{\left(\omega_k+2\tilde{\omega}\right)^2 - \omega_i^2} + \frac{e^{\mathrm{i}(\omega_k-2\tilde{\omega})T_0}}{\left(\omega_k-2\tilde{\omega}\right)^2 - \omega_i^2}\right] \\ & + 2\omega_0 \sum_{k=1,\ k\neq i}^{N} h_{ik}A_k\frac{e^{\mathrm{i}\omega_k T_0}}{\omega_k^2 - \omega_i^2} + \mathrm{cc}.\end{aligned} \tag{4.13}$$

Because there does not exist the case where $2\tilde{\omega}$ is simultaneously near $(\omega_{p,R} + \omega_{q,R})$ and $(\omega_{p,R} - \omega_{q,R})$, there is no unstable solution for (4.7). Hence the system is said to be always stable when $2\tilde{\omega}$ is away from $(\omega_{p,R} \pm \omega_{q,R})$.

5. Numerical Simulation and Discussion

To validate the reliability of the calculation methods in this paper, we first assumed that the angular speed of the rotating ER sandwich beam $\dot{\theta} = 0$ and regarded it as a static cantilever beam. The structural and material parameters of the beam in [19] were used to calculate the natural frequencies and modal loss factors for the first five orders when the electric field intensity $E = 3.5\,\mathrm{kV/mm}$. The results are shown in Table 1. We can see from the table that although the natural frequencies at each order obtained through the method in this paper

Table 1: Comparison of natural frequencies and loss factors obtained herein with those of [19] (L = 381 mm, b = 25.4 mm, $h_1 = h_3$ = 0.79 mm, h_2 = 0.5 mm, E = 3.5 kV/mm, $G_2^* = 612500(1 + 0.011\mathrm{i})$).

Mode	Natural frequency f (Hz)		Loss factor η	
	Present	Ref.	Present	Ref.
1	10.011	10.005	0.00393	0.00395
2	40.091	40.051	0.00507	0.00512
3	89.125	89.028	0.00459	0.00461
4	152.926	152.702	0.00336	0.00339
5	236.396	235.761	0.00244	0.00250

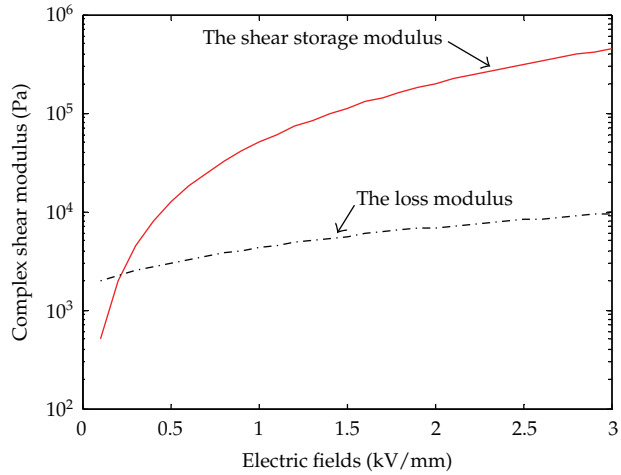

Figure 4: Complex shear modulus of ER fluids at different electric fields.

are slightly higher than that obtained from the Mead-Markus modeling method in [19], the difference is minimal. The loss factors obtained through the two methods are basically the same. We also used the geometric and material parameters of rotating beams at the active restraint damping layer in [26] to calculate the natural frequencies and modal damping ratio for the first two orders under different rotation speeds (Table 2) and found that the result obtained from the method in this paper is almost the same as that obtained from [26].

The effects of an electric field on the dynamic characteristics and parametric instability of the rotating ER sandwich beam were studied. The sandwich beam was constructed with an ER material core and two elastic faces made of aluminum. The material properties and geometrical parameters are shown in Table 3. The ER materials used in this study are same as those described by Don [27]. Its density is 1200 kg/m^2, and complex modulus can be expressed as

$$G^* = 50000E^2 + (2600E + 1700)\mathrm{i}, \tag{5.1}$$

where E is the electric fields in kV/mm. The shear storage modulus G_1 and the loss modulus G_2 are shown in Figure 4.

The dynamic characteristics of the rotating sandwich beam with an ER core were investigated first. Let the angular velocity of the rotating beam $\dot{\theta} = \dot{\theta}_0$. Then the natural frequencies and damping loss factors can be obtained by the eigenvalue equations

$$\left\{\left[\mathbf{K_1} + \dot{\theta}^2(\mathbf{K_2} - \mathbf{M})\right] - (\omega^*)^2[\mathbf{M}]\right\}\{\Phi\} = 0, \tag{5.2}$$

Table 2: Comparison of a rotating beam for natural frequencies and modal damping ratio obtained herein with those of [26] ($L = 300$ mm, $b = 12.7$ mm, $h_1 = 0.762$ mm, $h_3 = 2.286$ mm, $h_2 = 0.25$ mm, $G_2^* = 261500(1 + 0.38\mathrm{i})$).

Angular velocity $\dot{\theta}$ (r.p.m)		Natural frequency		Modal damping ratio	
		f_1 (Hz)	f_2 (Hz)	η_1^*	η_2^*
0	Ref.	20.15	104.0	0.0382	0.0235
	Present	20.14	103.9	0.0384	0.0233
600	Ref.	20.58	106.8	0.0365	0.0220
	Present	20.53	106.6	0.0366	0.0222
1000	Ref.	21.20	111.2	0.0340	0.0201
	Present	21.17	111.1	0.0340	0.0204

Table 3: Parameters of ER sandwich beam.

Parameters of beam geometry	$L = 300$ mm, $b = 20$ mm, $h_1 = h_3 = 0.5$ mm, $h_2 = 2$ mm
Elastic layer properties (Al)	$\rho_1 = \rho_3 = 2700\,\mathrm{kg/m^3}$, $E_1 = E_3 = 70$ Gpa
ER fluid properties [27]	$\rho_2 = 1200\,\mathrm{kg/m^3}$, $G^* = 50000E^2 + (2600E + 1700)\mathrm{i}$

where ω^* is the complex frequency (rad/s) and $\{\Phi\}$ is the corresponding eigenvector. The complex eigenvalue $\{\omega^*\}^2$ is expressed as

$$(\omega^*)^2 = \omega^2(1 + \mathrm{i}\eta), \tag{5.3}$$

where η is the damping loss factor and ω is the natural frequency.

Comparisons of the natural frequencies and loss factors of ER sandwich beams with different rotating speed are shown in Figures 5 and 6, respectively. Figure 5 shows the effects of electric field strength on the first three natural frequencies. It is observed that the increment of the electric field strength increases the natural frequencies of the ER sandwich beam at different rotation speeds. Thus, the stiffness of the rotating beam increases with the strength of the applied electric field. Figure 6 illustrates the effect of electric field strength on the loss factors. At all rotation speeds, the loss factor first increases as the electric field strength increases. But the loss factor declines with the strength of the electric field when the electric field strength exceeds 0.5 kV/mm. This trend is very obvious in lower modes and less evident in higher modes. Figures 5 and 6 also demonstrate that the natural frequency increases and the loss factor decreases with an increase in rotating speed. That is because the stiffness of the rotating ER beam increases with rotating speed, whereas its damping decreases with rotating speed. Thus the natural frequencies and loss factors of the rotating ER beam can be altered by varying the strength of the applied electric field.

The multiple scale method was used to obtain the parametric instability region of the rotating ER sandwich beam with periodically variable angular velocity. The effects of electric field strength on the region of parametric instability are shown in Figure 7. Figures 7(a) and 7(b) illustrate the instability regions for the first and second order parametrically excited resonance, respectively, and Figures 7(c) and 7(d) are the instability regions for parametrically excited combination resonance of sum and difference types. It is noted that increasing the electric field strength will increase the excitation frequency so that the unstable regions shift to the right. The critical maximal rotating speed (i.e., the maximal rotating speed when parametric instability occurs) increases and the width of unstable region decreases with an increase in the strength of the electric field. Thus increasing the strength of the applied

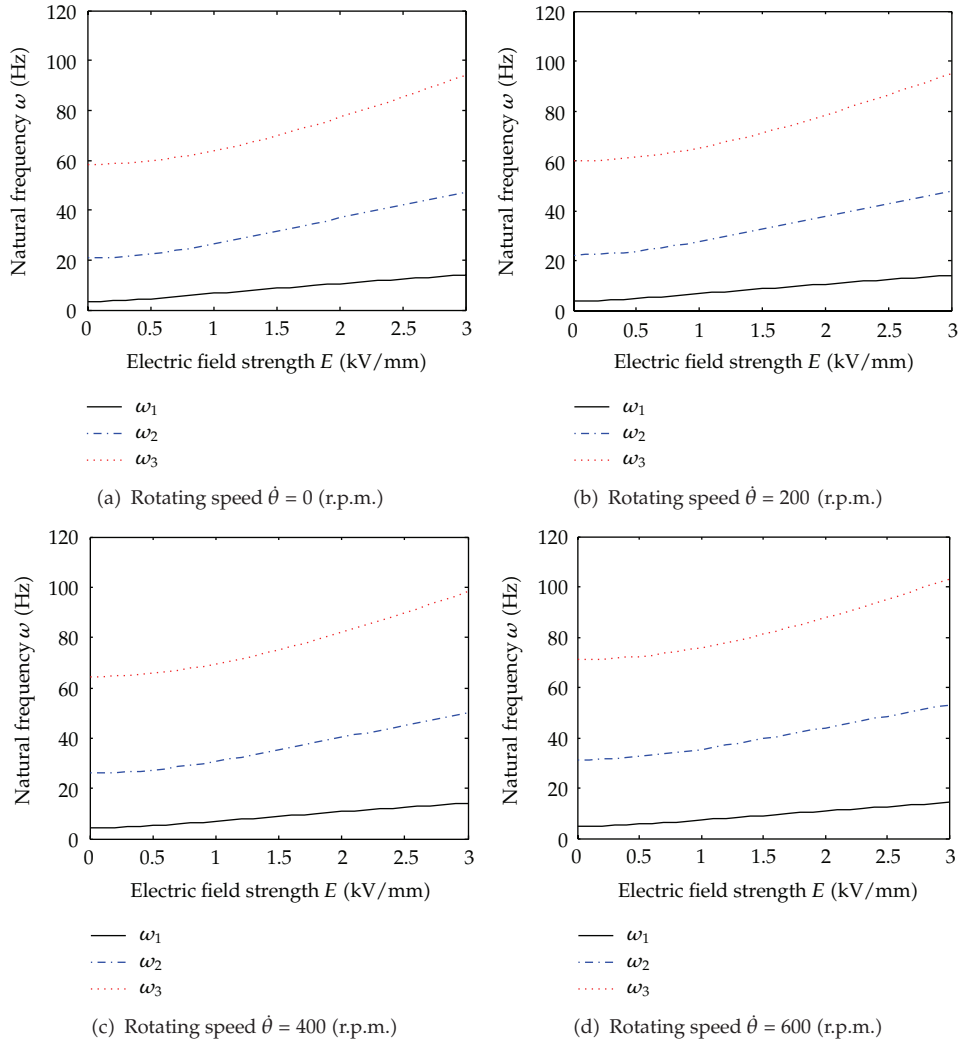

Figure 5: Effect of strength of electric field on the first three natural frequencies at different rotation speeds.

electric field not only moves the region of instability to a higher frequency, but also reduces the width of the region. That is, increasing the electric field strength will increase the stability of the beam.

The results of the stability analysis can be verified by investigating the time responses for points A and B in Figure 7(a). The time responses for the transverse displacement are computed at the free end of the ER sandwich beam by (3.18) using the fourth-order Runge-Kutta method. The co-ordinates of points A and B in Figure 7(a) are (0.8, 3) and (1, 3). As shown in Figure 7(a), point A is in the stable region and point B is in the unstable region without an applied electric field, whereas points A and B are both in the stable region when the electric field strength $E = 0.5\,\text{kV/mm}$.

Comparisons of the time responses of points A and B without electric field are shown in Figure 8. The time response for point A, as shown in Figure 8(a), is bounded by a limited value. However, for point B, which is within the unstable region, the amplitude of the time

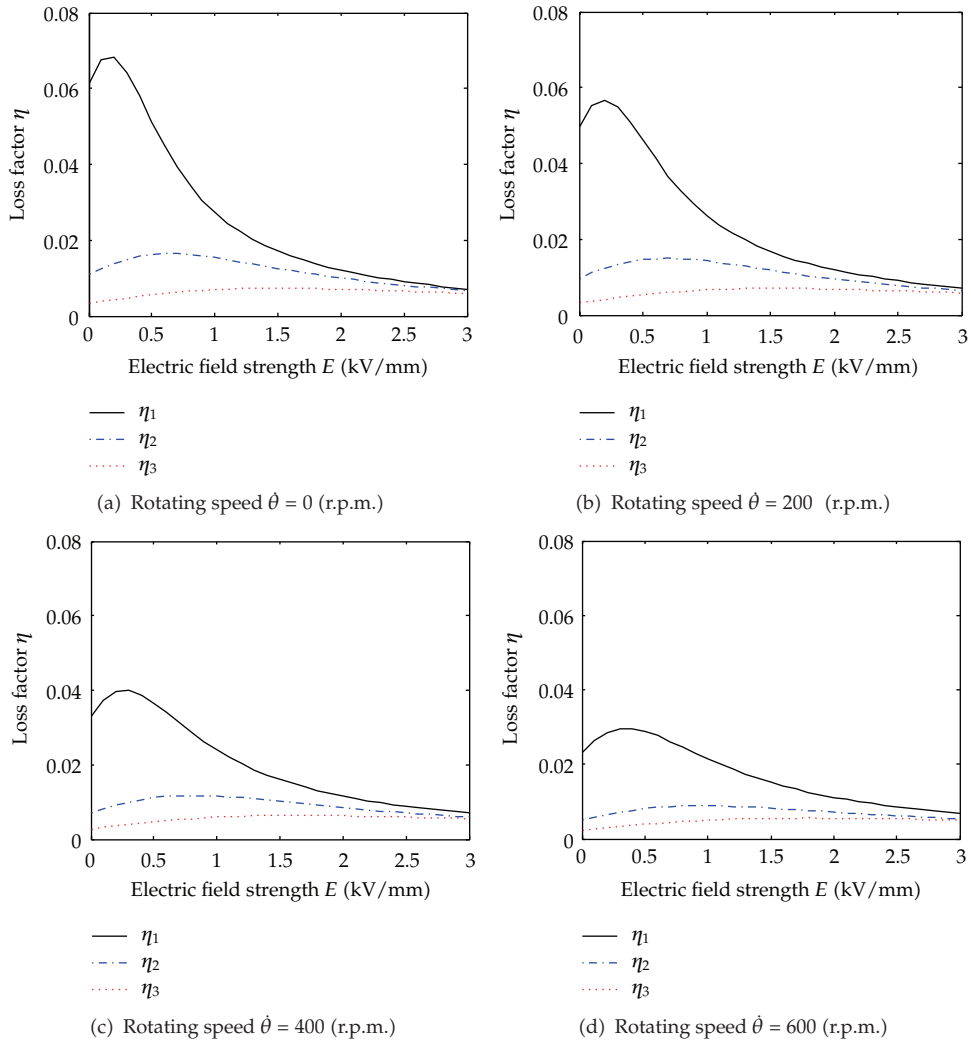

Figure 6: Effect of strength of electric field on the first three loss factors at different rotation speeds.

response increases with time, as illustrated in Figure 8(b). Figure 9 shows the time responses for points A and B when the electric field strength $E = 0.5\,\text{kV/mm}$. It is demonstrated that points A and B are both stable because the time responses are bounded. Therefore, it is verified that the stability results of Figure 7(a) agree well with the behavior of the time responses in Figures 8 and 9.

6. Conclusion

The dynamic characteristics and parametric instability of rotating ER sandwich beams with a periodically variable angular velocity were studied using FEM and a multi-scale method. The effects of electric field on the natural frequency, loss factor, and regions of parametric instability were investigated. When the strength of the electric field is increased, the stiffness of the ER sandwich beam increases at different rotation speeds and the instability region

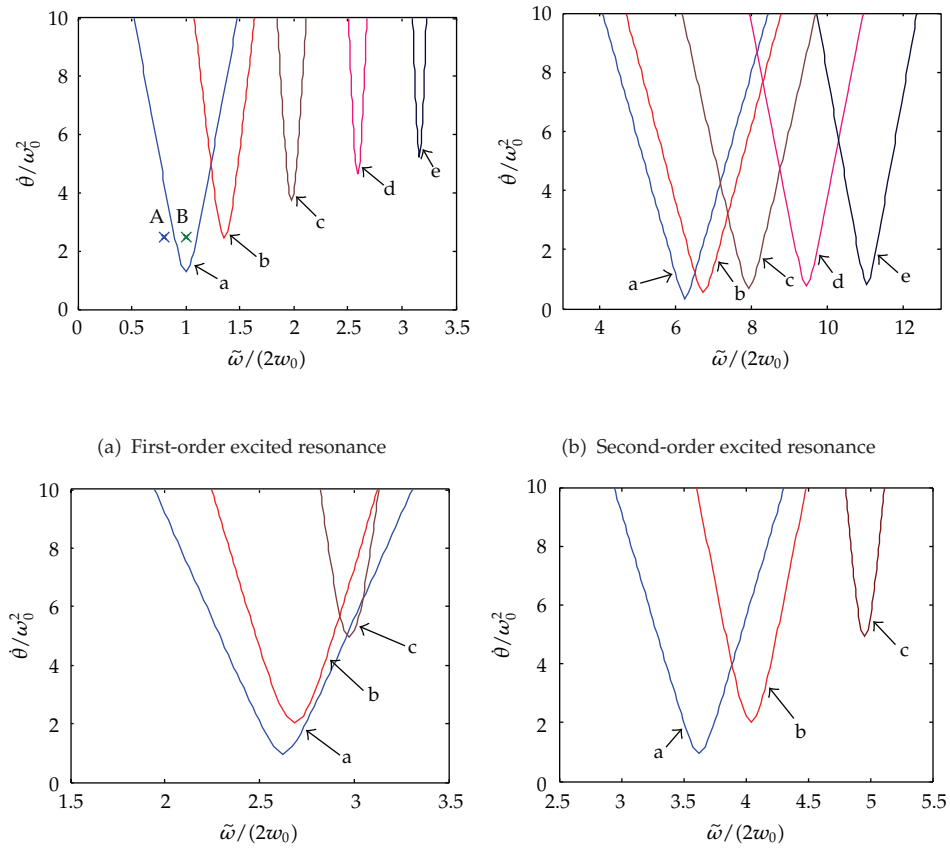

(a) First-order excited resonance

(b) Second-order excited resonance

(c) Combination resonance of difference types

(d) Combination resonance of sum types

Figure 7: Instability boundaries for various applied electric fields: curve a, $E = 0\,\text{kV/mm}$; curve b, $E = 0.5\,\text{kV/mm}$; curve c, $E = 1.0\,\text{kV/mm}$; curve d, $E = 1.5\,\text{kV/mm}$; curve e, $E = 2\,\text{kV/mm}$.

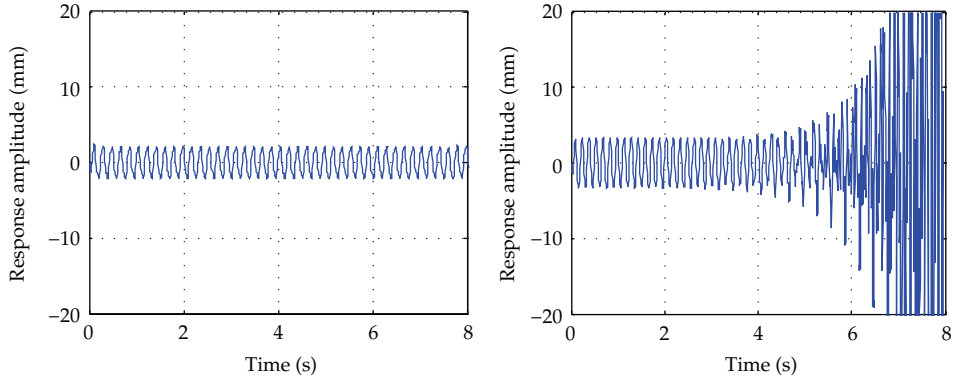

(a) Time responses of point A in Figure 7(a)

(b) Time responses of point B in Figure 7(a)

Figure 8: Time responses of the transverse displacement at electric field $E = 0\,\text{kV/mm}$.

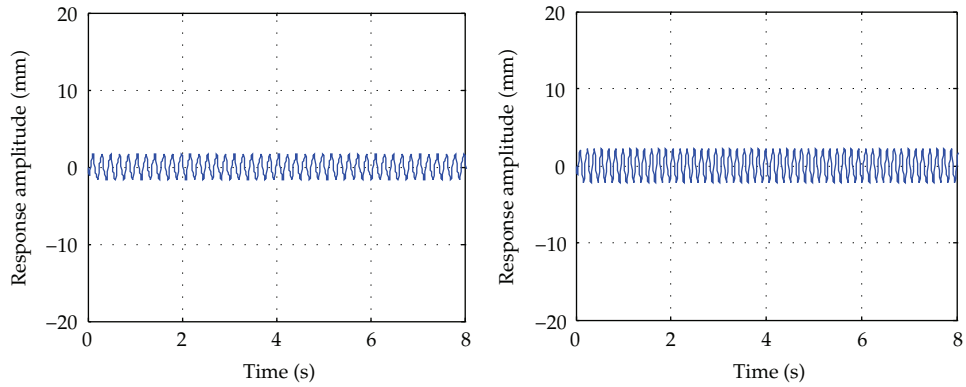

(a) Time responses of point A in Figure 7(a)

(b) Time responses of point B in Figure 7(a)

Figure 9: Time responses of the transverse displacement at electric field $E = 0.5\,\mathrm{kV/mm}$.

of the rotating beam moves toward the high-frequency section. The unstable regions narrow with an increase in the strength of the electric field, while the maximum critical angular speed required for the beam to have parametric instability increases as electric field increases. Hence the vibration characteristics and dynamic stability of rotating ER sandwich beams can be adjusted when they are subjected to an electric field. It was demonstrated that the ER material layer can be used to improve the parametric instability of rotating flexible beams.

Acknowledgments

This work was supported by the National Natural Science Foundation of China (11172100 and 51075138), and the Scientific Research Fund of Hunan Provincial Education Department of China (10A021).

References

[1] J. Chung and H. H. Yoo, "Dynamic analysis of a rotating cantilever beam by using the finite element method," *Journal of Sound and Vibration*, vol. 249, no. 1, pp. 147–164, 2002.

[2] A. A. Al-Qaisia, "Dynamics of a rotating beam with flexible root and flexible hub," *Structural Engineering and Mechanics*, vol. 30, no. 4, pp. 427–444, 2008.

[3] S. Y. Lee, S. M. Lin, and Y. S. Lin, "Instability and vibration of a rotating Timoshenko beam with precone," *International Journal of Mechanical Sciences*, vol. 51, no. 2, pp. 114–121, 2009.

[4] H. Arvin and F. Bakhtiari-Nejad, "Non-linear modal analysis of a rotating beam," *International Journal of Non-Linear Mechanics*, vol. 46, no. 6, pp. 877–897, 2011.

[5] B. A. H. Abbas, "Dynamic stability of a rotating Timoshenko beam with a flexible root," *Journal of Sound and Vibration*, vol. 108, no. 1, pp. 25–32, 1986.

[6] T. H. Young and T. M. Lin, "Stability of rotating pretwisted, tapered beams with randomly varying speeds," *Journal of Vibration and Acoustics, Transactions of the ASME*, vol. 120, no. 3, pp. 784–790, 1998.

[7] S. C. Sinha, D. B. Marghitu, and D. Boghiu, "Stability and control of a parametrically excited rotating beam," *Journal of Dynamic Systems, Measurement and Control, Transactions of the ASME*, vol. 120, no. 4, pp. 462–469, 1998.

[8] J. Chung, D. Jung, and H. H. Yoo, "Stability analysis for the flapwise motion of a cantilever beam with rotary oscillation," *Journal of Sound and Vibration*, vol. 273, no. 4-5, pp. 1047–1062, 2004.

[9] O. Turhan and G. Bulut, "Dynamic stability of rotating blades (beams) eccentrically clamped to a shaft with fluctuating speed," *Journal of Sound and Vibration*, vol. 280, no. 3–5, pp. 945–964, 2005.

[10] D. Younesian and E. Esmailzadeh, "Non-linear vibration of variable speed rotating viscoelastic beams," *Nonlinear Dynamics*, vol. 60, no. 1-2, pp. 193–205, 2010.

[11] K. Wei, G. Meng, W. Zhang, and S. Zhou, "Vibration characteristics of rotating sandwich beams filled with electrorheological fluids," *Journal of Intelligent Material Systems and Structures*, vol. 18, no. 11, pp. 1165–1173, 2007.

[12] M. V. Gandhi, B. S. Thompson, and S. B. Choi, "A new generation of innovative ultra-advanced intelligent composite materials featuring electro-rheological fluids: an experimental investigation," *Journal of Composite Materials*, vol. 23, no. 12, pp. 1232–1255, 1989.

[13] C. Y. Lee and C. C. Cheng, "Dynamic characteristics of sandwich beam with embedded electro-rheological fluid," *Journal of Intelligent Material Systems and Structures*, vol. 9, no. 1, pp. 60–68, 1998.

[14] T. Fukuda, T. Takawa, and K. Nakashima, "Optimum vibration control of CFRP sandwich beam using electro-rheological fluids and piezoceramic actuators," *Smart Materials and Structures*, vol. 9, no. 1, pp. 121–125, 2000.

[15] S. B. Choi, "Electric field-dependent vibration characteristics of a plate featuring an electrorheological fluid," *Journal of Sound and Vibration*, vol. 234, no. 4, pp. 705–712, 2000.

[16] J. Y. Yeh, L. W. Chen, and C. C. Wang, "Dynamic stability of a sandwich beam with a constrained layer and electrorheological fluid core," *Composite Structures*, vol. 64, no. 1, pp. 47–54, 2004.

[17] Z. F. Yeh and Y. S. Shih, "Critical load, dynamic characteristics and parametric instability of electrorheological material-based adaptive beams," *Computers and Structures*, vol. 83, no. 25-26, pp. 2162–2174, 2005.

[18] K. X. Wei, G. Meng, S. Zhou, and J. Liu, "Vibration control of variable speed/acceleration rotating beams using smart materials," *Journal of Sound and Vibration*, vol. 298, no. 4-5, pp. 1150–1158, 2006.

[19] M. Yalcintas and J. P. Coulter, "Electrorheological material based adaptive beams subjected to various boundary conditions," *Journal of Intelligent Material Systems and Structures*, vol. 6, no. 5, pp. 700–717, 1995.

[20] M. Yalcintas and J. P. Coulter, "Electrorheological material based non-homogeneous adaptive beams," *Smart Materials and Structures*, vol. 7, no. 1, pp. 128–143, 1998.

[21] E. H. K. Fung and D. T. W. Yau, "Vibration characteristics of a rotating flexible arm with ACLD treatment," *Journal of Sound and Vibration*, vol. 269, no. 1-2, pp. 165–182, 2004.

[22] H. Saito and K. Otomi, "Parametric response of viscoelastically supported beams," *Journal of Sound and Vibration*, vol. 63, no. 2, pp. 169–178, 1979.

[23] H. H. Yoo and S. H. Shin, "Vibration analysis of rotating cantilever beams," *Journal of Sound and Vibration*, vol. 212, no. 5, pp. 807–808, 1998.

[24] H. Y. Hu, *Applied Nonlinear Dynamics*, Press of Aeronautical Industries, Beijing, China, 2000.

[25] T. H. Tan, H. P. Lee, and G. S. B. Leng, "Parametric instability of spinning pretwisted beams subjected to spin speed perturbation," *Computer Methods in Applied Mechanics and Engineering*, vol. 148, no. 1-2, pp. 139–163, 1997.

[26] C. Y. Lin and L. W. Chen, "Dynamic stability of a rotating beam with a constrained damping layer," *Journal of Sound and Vibration*, vol. 267, no. 2, pp. 209–225, 2003.

[27] D. L. Don, *An investigation of electrorheological material adaptive structure [M.S. thesis]*, Lehigh University, Bethlehem, Pa, USA, 1993.